Accounting for the topology of road networks to better explain human-mediated dispersal in terrestrial landscapes

Charles Rocabert, Serge Fenet, Bernard Kaufmann, Jérôme Gippet

ECOGRAPHY

Research article

Accounting for the topology of road networks to better explain human-mediated dispersal in terrestrial landscapes

Charles Rocabert[1,2], **Serge Fenet**[3,4], **Bernard Kaufmann**[5] **and Jérôme M. W. Gippet**[5,6]

[1]Institute for Computer Science and Department of Biology, Heinrich-Heine-Universität, Düsseldorf, Germany
[2]INRIA, Lyon, France
[3]Équipe STEEP, Université Grenoble Alpes, CNRS, INRIA, Grenoble INP, LJK, Grenoble, France
[4]University of Lyon, Université Claude Bernard Lyon 1, CNRS, LIRIS, UMR5205, Villeurbanne, France
[5]University of Lyon, Université Claude Bernard Lyon 1, CNRS, ENTPE, UMR 5023 LEHNA, Villeurbanne, France
[6]Department of Ecology and Evolution, University of Lausanne, Lausanne Switzerland

Correspondence: Charles Rocabert (charles.rocabert@gmail.com); Jérôme M. W. Gippet (jgippet@gmail.com)

Ecography
2023: e07068
doi: 10.1111/ecog.07068
Subject Editor: Timothy Keitt
Editor-in-Chief: Miguel Araújo
Accepted 10 October 2023

Human trade and movements are central to biological invasions worldwide. Human activities not only transport species across biogeographical barriers, but also accelerate their post-introduction spread in the landscape. Thus, by constraining human movements, the spatial structure of road networks might greatly affect the regional spread of invasive species. However, few invasion models have accounted for the topology of road networks so far, and its importance for explaining the regional distribution of invasive species remains mostly unexplored. To address this issue, we developed a spatially explicit and mechanistic human-mediated dispersal model that accounts and tests for the influence of transport networks on the regional spread of invasive species. Using as a model the spread of the invasive ant *Lasius neglectus* in the middle Rhône valley (France), we show that accounting for the topology of road networks improves our ability to explain the current distribution of the invasive ant. In contrast, we found that using human population density as a proxy for the frequency of transport events decreases models' performance and might thus not be as appropriate as previously thought. Finally, by differentiating road networks into sub-networks, we show that national and regional roads are more important than smaller roads for explaining spread patterns. Overall, our results demonstrate that the topology of transport networks can strongly bias regional invasion patterns and highlight the importance of better incorporating it into future invasion models. The mechanistic modelling approach developed in this study should help invasion scientists explore how human-mediated dispersal and topography shape invasion dynamics in landscapes. Ultimately, our approach could be combined with demographic, natural dispersal and environmental suitability models to refine spread scenarios and improve invasive species monitoring and management at regional to national scales.

NORDIC SOCIETY OIKOS

www.ecography.org

Keywords: biological invasions, human-mediated dispersal, road network, secondary spread, spatially explicit model, stochastic jump model

Introduction

Biological invasions are a major cause of the current biodiversity crisis, cost billions in damages and control efforts, and contribute to the spread of zoonotic diseases (Bradshaw et al. 2016, Maxwell et al. 2016, Zhang et al. 2022). Human movements and trade are the primary cause of biological invasions (Hulme et al. 2008, Hulme 2009). By attaching to human transport vectors or by contaminating transported commodities, plants and animals are unintentionally transported over long distances (i.e. from a few hundred meters to thousands of kilometers) and can get introduced beyond the biogeographic barriers that constrain their natural distribution (Hulme 2009, Auffret et al. 2014, Gippet et al. 2019).

This dispersal process, termed human-mediated dispersal (HMD; Bullock et al. 2018), introduces species into new environments, but can also accelerate their post-introduction spread in the landscape. In addition to invasive species' natural dispersal abilities, a broad variety of human activities are involved in the spread of invasive species at the regional scales (hereafter 'regional spread'; Johnson et al. 2006). For example, seeds of invasive plants can be transported in mud stuck to hikers' shoes or car tires (Ansong and Pickering 2013, 2014). Major invertebrate pests such as the spongy moth *Lymantria dispar* or the emerald ash borer *Agrilus planipennis* are notoriously transported within firewood at distances up to two hundred kilometers (Johnson et al. 2006, Muirhead et al. 2006, Koch et al. 2012). The larvae of tiger mosquitoes *Aedes albopictus* are easily transported in water retained in used tires (Roiz et al. 2007) and adult tiger mosquitoes were found in cars traveling between major cities in Spain (Eritja et al. 2017). Human-mediated dispersal can even be the main driver of invasion success in invasive species with limited natural dispersal capabilities such as Argentine ants (*Linepithema humile*; Suarez et al. 2001), Japanese knotweeds (*Fallopia* spp.; Rouifed et al. 2014) or Zebra mussels (*Dreissena polymorpha*; Johnson et al. 2001). However, despite the abundant evidence supporting the prominent role of HMD in the regional spread of invasive species, this dispersal process is still poorly understood and modelled (Horvitz et al. 2017).

Human-mediated dispersal is difficult to describe, understand and predict because it involves frequent, diverse, and often inconspicuous human activities such as landscaping, tourism or commuting (Koch et al. 2012, Ansong and Pickering 2013, Auffret et al. 2014, Perkins et al. 2014). However, human activities are not occurring homogeneously or randomly across landscapes as they are more frequent in densely populated areas and strongly constrained by the topology (i.e. spatial structure) of transport networks (Von Der Lippe and Kowarik 2008, Banks et al. 2015). Therefore, the spatial heterogeneity of human activities and movements might greatly affect the spread of invasive species (Banks et al. 2015, Morel-Journel et al. 2018). Nevertheless, regional human-mediated dispersal models rarely account for the topology of the road network or the heterogeneity of human activities (Pitt et al. 2009, Roura-Pascual et al. 2009, Lustig et al. 2017, Robinet et al. 2018, Bagnara et al. 2022, Lee et al. 2022) and their importance for explaining the post-introduction spread of invasive species remains mostly unexplored.

To address this issue, we modelled the human-mediated dispersal of the invasive ant *Lasius neglectus* in the middle Rhône valley (France) and tested for the importance of accounting for the topology of the road network and for the intensity of human activities to explain *L. neglectus* post-introduction spread. The invasion of the ant *L. neglectus* in the middle Rhône valley provides an ideal system to study the influence of transport networks and human activities on human-mediated dispersal at regional scale. The invasive garden ant *L. neglectus* presumably originates from Asia Minor (Van Loon et al. 1990, Ugelvig et al. 2008) and has been recorded outside of its native range for the first time in 1973 in Hungary horticultural trade (Van Loon et al. 1990), and in 1995 in the middle Rhône valley (based on inhabitants' testimonies in the heavily infested village of Saint-Désirat). Genetic analyses suggested a unique introduction for all known French populations (Ugelvig et al. 2008). Like most invasive ant species, *L. neglectus* has limited natural dispersal abilities because its winged reproductive females do not perform nuptial flights (Espadaler et al. 2007). Natural dispersal only consists in the slow incremental expansion of colonies (20–100 m per year; Espadaler et al. 2007). Therefore, at landscape scale, the spread of this species occurs via human-mediated dispersal when contaminated materials such as soil or potted plants are transported for landscaping, construction, or horticultural trade (Van Loon et al. 1990, Schultz and Seifert 2005). Moreover, *L. neglectus* has no strong climatic limitation in the study region and is even predicted to be one of the less climatically limited invasive ants in France (Bertelsmeier and Courchamp 2014, Gippet et al. 2017). The combination of these two characteristics (i.e. limited natural dispersal and weak environmental limitations) suggests that the distribution of *L. neglectus* in the middle Rhône valley is mostly shaped by human-mediated dispersal.

Modeling human-mediated dispersal at a regional scale is challenging. While long-distance HMD is generally associated with easily identifiable ports of entry (i.e. transportation hubs such as seaports; Seebens et al. 2016), short-distance HMD mostly occurs in continuous space with no clear departure and arrival locations (e.g. private houses, road sides, unauthorized dump sites; Gippet et al. 2017). Nevertheless, several secondary spread models have included short-distance HMD, generally in the form of

gravity models (Bossenbroek et al. 2001, Prasad et al. 2010, Crespo-Pérez et al. 2011, McNitt et al. 2019) or stochastic jump models (Pitt et al. 2009, Savage and Renton 2014, Lustig et al. 2017). Gravity models estimate HMD among discrete locations (at long and short distance) based on the intensity of human activity and distance (Crespo-Pérez et al. 2011), and are useful when human activities occur across a network of well-defined hubs (e.g. airports, maritime ports, lakes, cities) and when information about human activities at and between these hubs is available (McNitt et al. 2019). However, these two conditions are rarely met, either because there are no clearly defined hubs involved in the human activity fostering dispersal, or because trade or travel volumes between locations are unknown (Robinet et al. 2016, Gippet et al. 2017, Suppo et al. 2018). Stochastic jump models overcome this limitation by modelling HMD events as random jumps in continuous space (Savage and Renton 2014). In addition, these models are mechanistic and thus have meaningful and easy to interpret dispersal parameters such as the number, distance and direction of HMD events (Dormann et al. 2012, Lustig et al. 2017). Stochastic jump models of HMD in insects and plants often use the density of human population (or an equivalent index of the intensity of human activities) to determine the number of HMD events happening each year and their heterogeneity across space. For example, cities are expected to import and export more alien species because they concentrate human activities (Robinet et al. 2018). However, existing stochastic jump models underestimate the importance of the transportation networks as they are typically isotropic: dispersal events have identical probabilities of going in any direction (Pitt et al. 2009, Lustig et al. 2017, Robinet et al. 2018).

Using a stochastic jump model approach, we developed a spatially explicit and mechanistic HMD model that allows to account and test for the influence of the intensity of human activities and the topology of transport networks on the regional spread of invasive species. Our modelling approach consists in a constrained random-walk model using a simplified representation of the road network to simulate directionally biased HMD events in terrestrial landscapes.

Material and methods

Study area, road network topology and human activity index

The study area includes the city of Lyon (France) and its surrounding urban area (~16 000 km^2; Fig. 1). As the second most populated urban area in France with more than two million inhabitants, it is an important road transportation hub with six major motorways (A6, A7, A42, A43, A47 and A89) converging to Lyon. A heterogeneous secondary road network covers the area, constrained by mountain ranges and most developed along the Rhône and Saône rivers. The study area was discretized in a regular tessellation composed of 3944 square cells of 2 × 2 km (Fig. 1, grey grid; Supporting information). This cell size provided a good trade-off between simplification and precision, given the extent of the study area.

The road network of the study area was compiled from the French National Institute of Geographic and Forest Information (www.ign.fr) public database (Fig. 1a; BD TOPO® 2013 available at www.geoportail.gouv.fr). We used four out of six road categories provided by the database

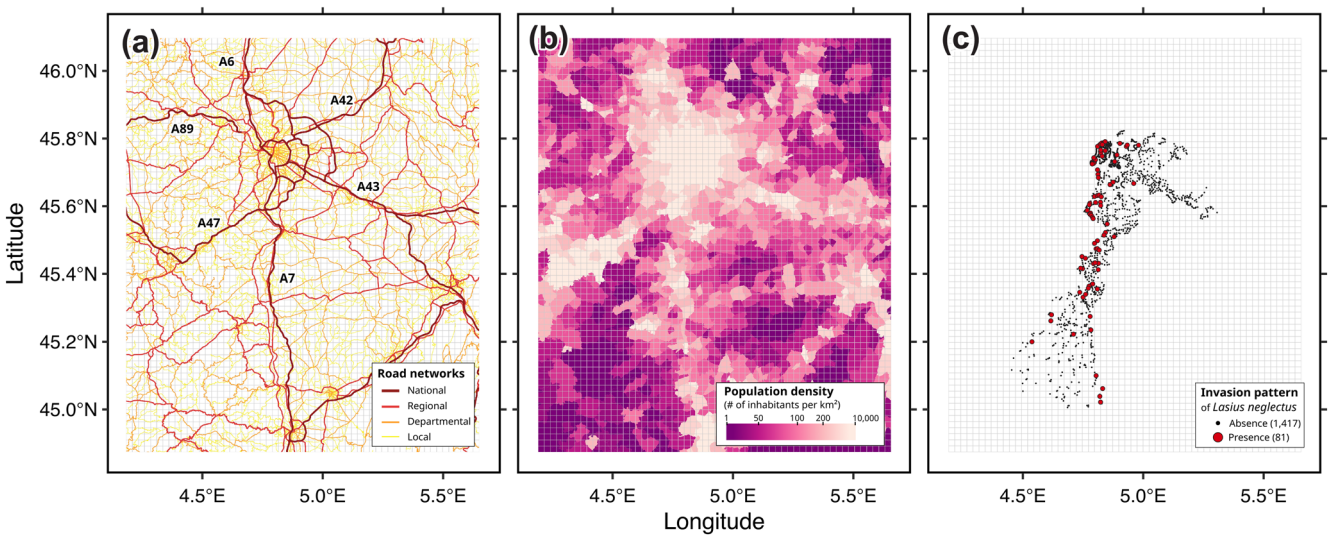

Figure 1. Study area (the middle Rhône valley) discretized with a regular tessellation of 2 × 2 km cells (grey grid). (a) Road network composed of four road categories. Lyon city is the main transport hub in this area. Highways A89, A6, A42, A43, A7 and A47 (in dark red) are labeled (b) Population density. This measure is used in the model as a proxy for the frequency of human-mediated dispersal events. (c) Distribution of the invasive ant *L. neglectus* in the study area according to a standardized survey of 1498 sampled locations. The modelling area (grey grid) is substantially larger than the sampled area to limit border effects associated with out-of-the-map dispersal events during simulations.

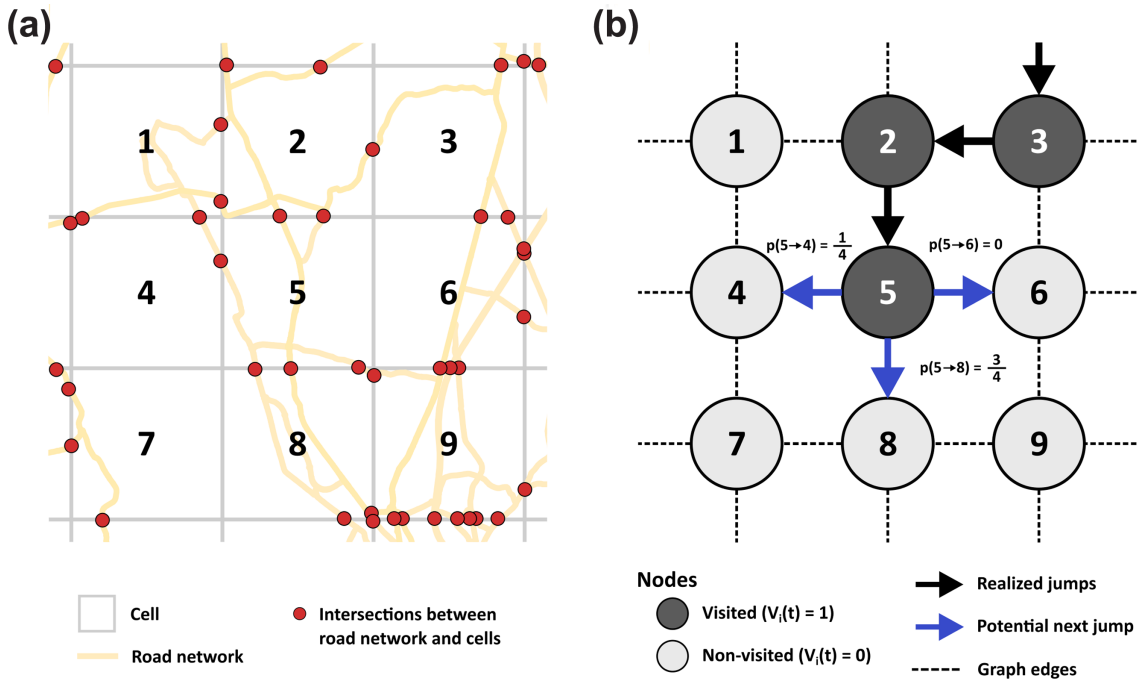

Figure 2. Using the topology of the road network to bias the direction of dispersal events. (a) The study area is discretized in a regular tessellation of 2 × 2 km squares (numbered from 1 to 9 in this example). The tessellation (grey grid) intersects the road network (yellow lines) in several locations (red dots). (b) Undirected and weighted graph corresponding to the discretization on panel (a). Nodes 1 to 9 (black circles) are connected by edges weighted by the sum of road intersections (Eq. 1). In this example, we consider only one road category of weight 1. A self-avoiding random walk (i.e. one HMD event) is ongoing (black arrows), and a jump must be computed from the node 5 to a neighbor cell. Nodes 2, 3 and 5 (in dark grey) have already been visited during the current random walk and cannot be visited again ($V_2(t) = V_3(t) = V_5(t) = 1$). Blue arrows symbolize the allowed directions of the future jump, with associated probabilities. The probability to jump into cell 2 is zero, because it has already been visited. The probability to jump into cell 6 is also zero, because no road connects cells 5 and 6.

according to their importance for human movements at different spatial scales: 1) national; 2) regional; 3) departmental and 4) local. Smaller road categories (5 and 6) were discarded because they are not always passable for motor vehicles (e.g. hiking trails or stairs) and are thus irrelevant for human activities involved in soil transport. We then computed the cell-to-cell road connectivity graph ('Description of the human-mediated dispersal modelling framework' and Fig. 2 for details) using ArcGIS 10.1® (www.esri.com/software/arcgis).

As a measure of the frequency of human-mediated dispersal events per year, we used human population density per cell (i.e. the number of inhabitants by square kilometers; source: French National Institute of Geographic and Forest Information; Fig. 1b; Supporting information). This metric is commonly used as a proxy of the amount of human activities in modelling studies (Robinet et al. 2009, Crespo-Pérez et al. 2011).

Presence/absence dataset

We used a presence/absence dataset from an extensive sampling survey designed to detect the invasive ant *L. neglectus* in the middle Rhône valley (Fig. 1c). A total of 1498 locations were sampled between May and September in 2011, 2012, 2013 and 2015. Sampling locations were selected on public land with vegetation (an essential requirement for ant nests and foraging) wherever access was possible. Sampling locations were separated by at least 200 m in dense urban areas and by at least 500 m in suburban, residential and rural areas. Sampling was performed by teams of two to five persons for a combined search time of 40 min (sampling time depended on the number of samplers, for example, four samplers took 10 min per site; two samplers, 20 min per site) within a radius of 15–20 m, and only when air temperatures were comprised between 16 and 28°C (i.e. best detection condition according to Seifert 2007). Sampling consisted in a direct search of ant nests and trails on the ground, trees and shrubs, followed by hand collecting using an entomological aspirator. *Lasius neglectus*, like most other invasive ant species, forms large conspicuous populations of interconnected nests and, in spring and summer, thousands of workers are recruited on foraging trails that are easy to detect on trees, shrubs and on the ground, even by non-specialist observers (Gippet et al. 2018, Espadaler and Bernal 2020). In addition, to make sure that small *L. neglectus* populations were not confused with native *Lasius* species (typically *L. alienus*), all ants from the genus *Lasius* were sampled (one sample corresponds to one nest or one foraging trail) and identified to the species level in the lab (Seifert 2007).

Lasius neglectus was detected in 81 of the 1498 sampled locations (5.4% of sampled locations; Fig. 1c). For each cell of the discretized map, we calculated the total number of sampling locations and the number of sampling locations where *L. neglectus* was detected (Supporting information). A total of 362 cells contained at least one sampling location (mean ± s.d. = 4.1 ± 4.6 sampling locations per cell) and 56 cells (15.5% of the sampled cells) contained at least one invaded location (Fig. 1c). We also used a modelling area substantially larger than the sampled area (grey grid on Fig. 1c) to limit border effects associated with out-of-the-map dispersal events during simulations.

Description of the human-mediated dispersal modelling framework

To model the human-mediated dispersal of *L. neglectus* in the middle Rhône valley we developed a forward-in-time spatially explicit constrained random-walk modelling framework. We chose this approach because it allows to model human-mediated dispersal in continuous space and in a mechanistic way (Pitt et al. 2009, Savage and Renton 2014, Lustig et al. 2017). Mechanistic models provide ecologically sound parameters which are easy to interpret and thus, can offer direct information about the process being modelled, contrary to phenomenological/statistical models (e.g. gravity models, Crespo-Pérez et al. 2011). Moreover, our modelling approach brings two main novelties compared to previous spatially explicit mechanistic human-mediated dispersal models: first, each dispersal event consists of a self-avoiding random walk, instead of a single stochastic jump. Second, each step of the random walk is directionally biased according to the connectivity graph representing the topology of the road network (Fig. 2, 'Study area, road network topology and human activity index').

In our modelling framework, HMD is controlled by up to ten parameters: 1) T, the number of years after the initial introduction, 2) (x_0, y_0), the spatial coordinates of initial introduction (in meters from the bottom left corner of the map), 3) λ, the mean number of human-mediated dispersal events per year, 4) μ and σ^2, the mean and variance of the log-normal distribution of dispersal event distances (in number of cells, see below), and 5) r_1, r_2, r_3 and r_4 the weights associated to the four road categories presented above, which determine their relative contribution in biasing the direction of HMD events at each step of the random walks.

The model relies on a graph representing a coarse-grained version of the road network. To obtain this graph, the study area is discretized in a regular tessellation which is then intersected by the road network ('Study area, road network topology and human activity index', Fig. 2). Every road crossing a border between two neighbor cells (in the von Neumann neighborhood, see Fig. 2) constitutes a connection between them, generating an undirected and weighted graph (Fig. 2b). The absolute weight w_{ij} between two adjacent cells i and j is then the weighted sum of connecting roads by category:

$$w_{ij} = \sum_{k=1}^{4} r_k \times \mathrm{n}_{ijk}, \tag{1}$$

with r_k the weight of the road category k, and n_{ijk} the number of roads of category k connecting cells i and j. Map borders are absorbing, meaning that HMD events reaching a border are discarded.

Each cell i is characterized by a presence/absence status $S_i(t) \in \{0; 1\}$, 0 and 1 symbolizing the simulated absence or presence of the species, respectively. To reduce model complexity and the number of parameters to optimize (below), we assume that there is no mortality in the model: for example, the species is present in the initial introduction cell at all times ($S_0(t) = 1, \forall\, t$). After the initial introduction of the invasive species at $t = 0$, three steps drive the simulated HMD:

1. At each year t and for each cell i, the number of dispersal events $J_i(t)$ follows a Poisson distribution of parameter λ (the mean number of dispersal events per cell per year), weighted by an index of human activity h_i and the presence/absence status $S_i(t)$:

$$p\left(J_i\left(t\right)\right) \sim P\left(S_i\left(t\right) \times h_i \times \lambda\right). \tag{2}$$

If $S_i(t) = 0$ (absence of the species), there is no dispersal event in cell i at year t. h_i is the human activity index of cell i normalized by the maximum human activity index in the map $h_{\max}$.

$$\frac{h_i}{h_{\max}}. \tag{3}$$

2. At each year t and for each cell i, $J_i(t)$ dispersal events are computed. Each dispersal event is a self-avoiding random walk of length d following a log-normal distribution of mean μ and variance σ^2 (in number of cells traveled). In this study, we chose to use a log-normal distribution to model the distance of HMD events because it has been shown to fit observations of human travels at regional to continental scales (Koch et al. 2012, Adnan et al. 2021). Because the random walk is self-avoiding, each cell i has a temporary status $V_i(t) \in \{0; 1\}$, indicating if the cell has been visited during the current random walk ($V_i(t) = 1$) or not ($V_i(t) = 0$). During a random walk, the probability to jump from cell i to one of the four neighbor cells j follows:

$$p\left(i \to j\right) = \frac{w_{ij} \times \left(1 - V_j\right)}{\sum_{k=1}^{4} w_{ik} \times \left(1 - V_k\right)}; V_i = 1. \tag{4}$$

$V_i = 1$ indicates that the visiting status of cell i is set to 1. At the end of the random walk, the presence/absence status of the last visited cell is set to 1, ending the dispersal event. During a random walk, if all the neighbors of the current cell i are visited (i.e. $p(i \longrightarrow j) = 0, \forall\, j \in [1; 4]$),

the random walk stops at cell i, and $S_i(t)=1$. If a walk reaches a map border, the dispersal event is not accounted for in the simulation. At each new random walk, the visited status is reset to zero for all cells. Using this methodology, the direction of dispersal events only depends on the structure of the road network.

3. At the end of each simulation (when $t=T$), the model returns one presence/absence status $S_i(T)$ per cell i. To estimate the distribution of presence probabilities for a given set of parameters, it is thus necessary to run N independent stochastic simulations. The frequency $f_i(T)$ of the simulations that led to an invasion is computed for each cell i reads:

$$f_i(T)=\frac{\sum_{j=1}^{N} S_{ij}(T)}{N}, \tag{5}$$

with $S_{ij}(T)$ the presence/absence status of cell i in simulation j. The algorithm of the modelling framework is presented in Supporting information.

Testing the importance of road networks and human activities

Models comparison

Both the spatial heterogeneity in human activities and the topology of the road network can introduce anisotropy in HMD dynamics. To evaluate their impact on our ability to explain the invasion of *L. neglectus* in the middle Rhône valley, we compared four models: 1) an *isotropic* model, that does not account for any source of anisotropy, and is used as a null model, 2) a *human activity* model, that accounts only for the amount of human activities across the landscape, 3) a *road network* model, that accounts only for the topology of the road network, and 4) a *combined* model, that accounts for both sources of anisotropy.

For the *isotropic* model, both sources of anisotropy are ignored. The weight between every pair of adjacent cells i and j is $w_{ij}=1$, thus, there is no anisotropy due to the road network, and road category weights w_1 to w_4 are ignored. All cells are attributed the same human activity index (i.e. the mean human activity index in the study area). For the *human activity* model, only the spatial heterogeneity in human activities is considered (each cell has a specific human activity h_i, see Eq. 3). For the *road network* model, only the topology of the road network is considered. The weight between every pair of adjacent cells i and j is calculated considering the four road categories (Eq. 1). All cells are attributed the same human activity index (i.e. the mean human activity index in the study area). For the *combined* model, both sources of anisotropy are accounted for.

Dispersal parameters estimation

Based on previous knowledge on *L. neglectus* invasion history ('Presence/absence dataset'), we assumed that a single introduction event occurred 25 years ago, leading to a simulation time $T=25$ years. All the other parameters of the models (including the location of the initial introduction) were estimated by log-likelihood minimization based on the observed distribution of *L. neglectus* in the study area, using the minimization algorithm CMA-ES (Hansen et al. 2003). To compute the likelihood of a simulation, we used the hypergeometric law (Fisher's exact test for low sample sizes; Fisher 1935). Compared to the binomial likelihood, Fisher's exact test is more accurate for low counts and when the marginal sum is very imbalanced. Moreover, the hypergeometric likelihood (Eq. 6) naturally takes into account the sampling effort N_{obs} (the total number of sampling events per cell), as uncertainty decreases when the sampling effort increases, therefore giving more importance to cells with a higher sampling effort during the minimization of the log-likelihood. At the end of each simulation with N repetitions, the likelihood $L(i)$ of the simulation in each cell i then reads:

$$L(i)=\frac{\binom{n_1}{y_{sim}}\binom{n_2}{N-y_{sim}}}{\binom{n_1+n_2}{N}}, \tag{6}$$

with $n_1=y_{sim}+y_{obs}$, $n_2=(N-y_{sim})+(N_{obs}-y_{obs})$, and y_{sim} and y_{obs} the number of simulated and observed presences in cell i respectively. The log-likelihood l_{tot} of the simulation is the sum of negative log-likelihoods:

$$l_{tot}=-\sum_{i=1}^{m}\ln L(i), \tag{7}$$

with m the total number of cells with $N_{obs}>0$ (cells with no experimental sampling are not evaluated). The log-likelihood landscape being multi-dimensional and noisy due to the highly stochastic nature of the simulations, we applied a restart strategy and performed 1000 log-likelihood minimizations to increase the probability of finding the best solution (leading to approximately 4×10^{10} independent stochastic simulations, see Supporting information). For each model, we selected the parameters set having the lowest average log-likelihood score over 100 repetitions, meaning that this set of parameters is located at the highest calculated mean likelihood optimum. Mathematical terms are summarized in Table 1; model parameterization in Table 2.

Models performance comparison

We compared the four calibrated models using the Akaike information criterion (AIC) as the models differ in their number of parameters. Because our modelling framework is stochastic, a model's output, and thus performance, can vary across simulations. Thus, 100 repetitions were performed and the distributions of AIC values among models were compared

Table 1. Model parameters and mathematical variables.

Variable notation	Description
n	Number of independent stochastic simulations (here, n = 1000)
T	Total duration of the simulation after the initial introduction in years (here, $T = 25$)
(x_0, y_0)	Coordinates of the cell of initial introduction of the invasive species (coordinates of the cell centroid in meters)
λ	Mean number of dispersal events per cell per timestep (parameter of a Poisson distribution)
μ, σ^2	Mean and variance of the probability distribution (log-normal distribution) of the distance of dispersal events in number of cell-to-cell jumps
r_1, r_2, r_3, r_4	Road category weights
h_i	Human activity index of cell i
h_{max}	Maximum human activity index in the map
$S_i(t)$	Presence/absence status of cell i at time t ($S_i(t) \in \{0, 1\}$), 0 and 1 symbolizing the simulated absence or presence of the species, respectively
$J_i(t)$	Number of dispersal events of cell i at time t
$f_i(t)$	The frequency of the simulations that led to an invasion in cell i
y_{obs}, n_{obs}	Number of samples positive to *L. neglectus* y_{obs} and total samples n_{obs} in the observed dataset for a given cell
y_{sim}, n_{sim}	Number of repetitions invaded by *L. neglectus* y_{sim} and total number repetitions n_{sim} in the simulation dataset
$L(i)$	Hypergeometric likelihood of cell i
l_{tot}	Total negative log-likelihood of a model

using pairwise Wilcoxon tests with p-values adjusted for multiple comparisons.

To have a more detailed understanding of the performance of the models, we also computed five classical performance assessment metrics. 1) First, we computed the area under the receiver operator characteristic (ROC) curve (AUC), which evaluates the ability of the model to classify presences and absences (an AUC of 1 indicates perfect fit, 0.5 random fit and 0 perfect inverse fit; Hanley and Mcneil 1982) and is obtained by selecting the threshold value that maximizes both 2) the sensitivity (true positive rate) and 3) the specificity (true negative rate; Hosmer et al. 2013). Here, the threshold value used to binarize the simulation dataset is the simulated frequency of invaded cells $f_i(T)$ at the end of a simulation (Table 1). *Lasius neglectus* is considered present in a cell i if $f_i(T)$ is above the threshold (only cells with at least one experimental sample are evaluated). Next performance metrics were computed after having selected the threshold value that maximizes them specifically: 4) the F1 score, which evaluates the ability of a model to predict presences, in term of precision (i.e. proportion of true presences among simulated presences) and recall (i.e. sensitivity); and 5) the true skill statistic (TSS), which is an improvement of the Kappa score, reducing prevalence biases (Allouche et al. 2006). Values close to 1 indicate that the model accurately classify presences/absences.

These performance assessment metrics are based on a binary interpretation of the simulation results. To do so, we assumed that, among cells with at least one sampling location (362 cells), cells containing one or more invaded locations of the species were invaded (56 cells), and cells with no invaded location were non-invaded (306 cells). However, our optimization algorithm relies on a likelihood measure that depends on the sampling effort in each cell. Thus, for the likelihood, a cell containing many sampling locations will have more weight than a cell with only a few sampling locations. This is not reflected in the binary projections of the experimental sampling, which explains why cell-based performance metrics differ slightly from AIC in their assessment of the best model. Yet, these metrics are helpful to evaluate the quality of models in a generalizable way.

Results

The *road network* model was better at explaining observed invasion patterns than all other models (AIC ± SE = 324.55 ± 0.24; Table 3, Fig. 3, see Supporting information for log-likelihood distributions). Removing any source of anisotropy decreased model's performance (ΔAIC = 14.95; Table 3) as well as adding human activity (ΔAIC = 15.65; Table 3).

Table 2. Parameterization of the four HMD models. For each optimizable parameter, the range of allowed values is provided. Parameters are described in Table 1.

Parameters	(i) Isotropic model	(ii) Human activity model	(iii) Road network model	(iv) Combined model
n	1000 independent stochastic simulations			
T	25 years			
(x_0, y_0)	$x_0 \in [20\,000; 80\,000]$ and $y_0 \in [14\,000; 104\,000]$			
λ	$\lambda \in [0; 30]$			
μ, σ	$\mu \in [0; 30]$ and $\sigma \in [0.1; 3]$			
$r_1 \ldots r_4$	∅	∅	$r_i \in [0; 1]$	$r_i \in [0; 1]$
Human activity index h_i	Homogeneous h_i = mean (pop.dens.)	Heterogeneous	Homogeneous h_i = mean (pop.dens.)	Heterogeneous
Nb of estimated parameters k	5	5	9	9

Table 3. Parameter values for each calibrated model. Mean and SE of the log-likelihood and AIC over 100 repetitions. The difference with the AIC of the best model (i.e. the *road network* model) is computed from the mean AIC of each model. The best model is highlighted in green. Road weights are normalized to sum up to 1.

Parameters	(i) Isotropic model	(ii) Human activity model	(iii) Road network model	(iv) Combined model
Mean log-likelihood ± SE	164.75 ± 0.16	174.48 ± 0.17	153.28 ± 0.12	161.10 ± 0.14
Mean AIC ± SE	339.50 ± 0.31	358.97 ± 0.33	324.55 ± 0.24	340.20 ± 0.29
ΔAIC (based on mean AIC)	14.95	34.42	–	15.65
x_0	20026.56	29673.02	31238.47	60764.4
y_0	73514.26	58030.17	66451.83	38009.8
λ	17.15	26.92	13.14	22.56
μ	3.26	3.26	3.80	7.59
σ	1.59	0.82	2.41	0.16
r_1	–	–	0.36	0.81
r_2	–	–	0.59	0.12
r_3	–	–	0.049	0.056
r_4	–	–	0.0058	0.014

Considering human activity alone led to the worst model (ΔAIC = 34.42; Table 3).

According to the AUC metric (Fig. 4a), the *road network* (mean AUC ± SE = 0.808 ± 5.58 × 10^{-4}) and the *combined* (mean AUC ± SE = 0.809 ± 5.50 × 10^{-4}) models are the best to classify the observed data, but are not significantly different from each other. Binary classifiers with AUC values higher than 0.8 are generally assumed to be good (Hosmer et al. 2013). The *combined* model has a significantly higher sensitivity (mean sensitivity ± SE = 0.925 ± 4.70 × 10^{-3}; Fig. 4b) while the *road network* model has the highest specificity (mean specificity ± SE = 0.724 ± 1.41 × 10^{-2}; Fig. 4c). According to the F1 score (Fig. 4d), the road network model also performs better at predicting true positives (invaded cells) while minimizing the rate of false positives (mean F1 score ± SE = 0.507 ± 1.20 × 10^{-3}). Noticeably, according to the true skill statistic index (TSS; Fig. 4e), the *combined* model has the best performance (mean TSS ± SE = 0.534 ± 1.51 × 10^{-3}). See Supporting information for detailed model performance and Supporting information for detailed spatial distribution of observed and simulated presences/absences.

Each calibrated model differed in parameter values, including in the location of the initial introduction. This generated very different spatial distributions of simulated probability of presences at 25 years (Fig. 5).

A detailed explanation of the invasion dynamics of the *road network* model can be found in Supporting information. The simulation framework, the results and the pipeline to reproduce post-analyses and figures are available in Supporting information.

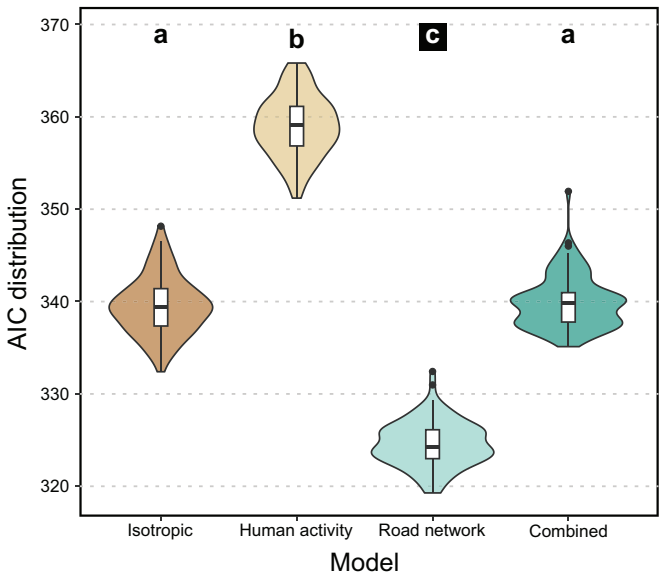

Figure 3. AIC distributions of each calibrated model. To obtain the distributions, 100 independent simulations were computed. Boxplot letter labels indicate result of pairwise Wilcoxon significance tests, with a Bonferroni correction of n = 6 (for the six pair-wise tests). The *isotropic* and *combined* models are not significantly different (p-value = 0.41). All other pairwise tests are significant with a p-value < 2.2 × 10^{-16}. The color of each violin plot corresponds to one model, as shown in the legend.

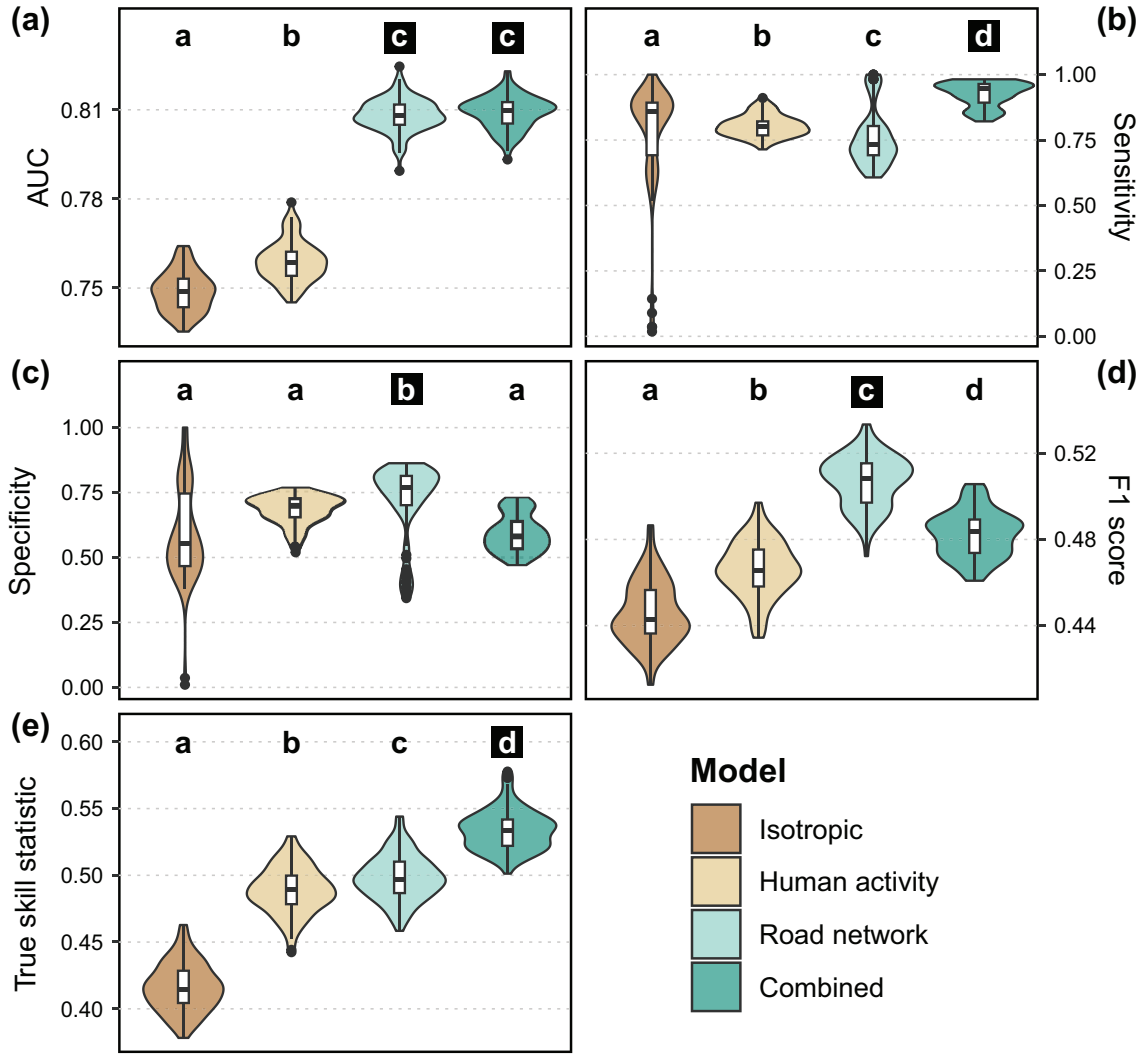

Figure 4. Performance metric distributions of each calibrated model. To obtain the distributions, 100 independent simulations were computed. Boxplot letter labels indicate pairwise Wilcoxon significance tests, with a Bonferroni correction of n = 6 (for the six pair-wise tests). For each metric, best(s) model(s) letters are highlighted in black. (a) AUC; (b) sensitivity; (c) specificity; (d) F1 score; (e) true skill statistic. The mean and the SE of the performance metrics of the four selected models are also summarized in Supporting information.

Discussion

We have shown that accounting for the topology of the road network in human-mediated dispersal models improved our ability to explain the spread of the invasive ant *L. neglectus* in the middle Rhône valley. The importance of the topology of transport networks in the post-introduction spread of invasive species has been increasingly discussed over the last decade but rarely tested (Auffret et al. 2014, Banks et al. 2015, Bullock et al. 2018, Gippet et al. 2019), and its integration in regional invasion models remains rare (Bagnara et al. 2022, Lee et al. 2022). Therefore, this study provides a valuable assessment of the importance of accounting for road networks topology to model and understand the regional spread of invasive species (Fig. 3–5). Interestingly, according to AIC (Fig. 3) and most other performance metrics used to compare the four models (i.e. *isotropic*, *road network*, *human activity* and *combined* models), the *road network* model was the best at explaining the regional distribution of *L. neglectus* in the study area (Fig. 4; Supporting information). However, some performance metrics gave a more nuanced result. The road network model and the combined model performed equally well according to AUC (0.81) and the combined model performed best according to the true skill statistic. These discrepancies among metrics give a richer picture of model performance as each metric represents a different aspect of the fit between simulated and observed invasion patterns. However, discrepancies might also result from the fact that, contrary to other performance metrics, AIC penalizes for model's complexity to avoid over-fitting, and also accounts for the sampling effort so that well sampled cells are given more weight than poorly sampled ones. More generally, we show that taking into account the structure of the road network significantly improves model performance in

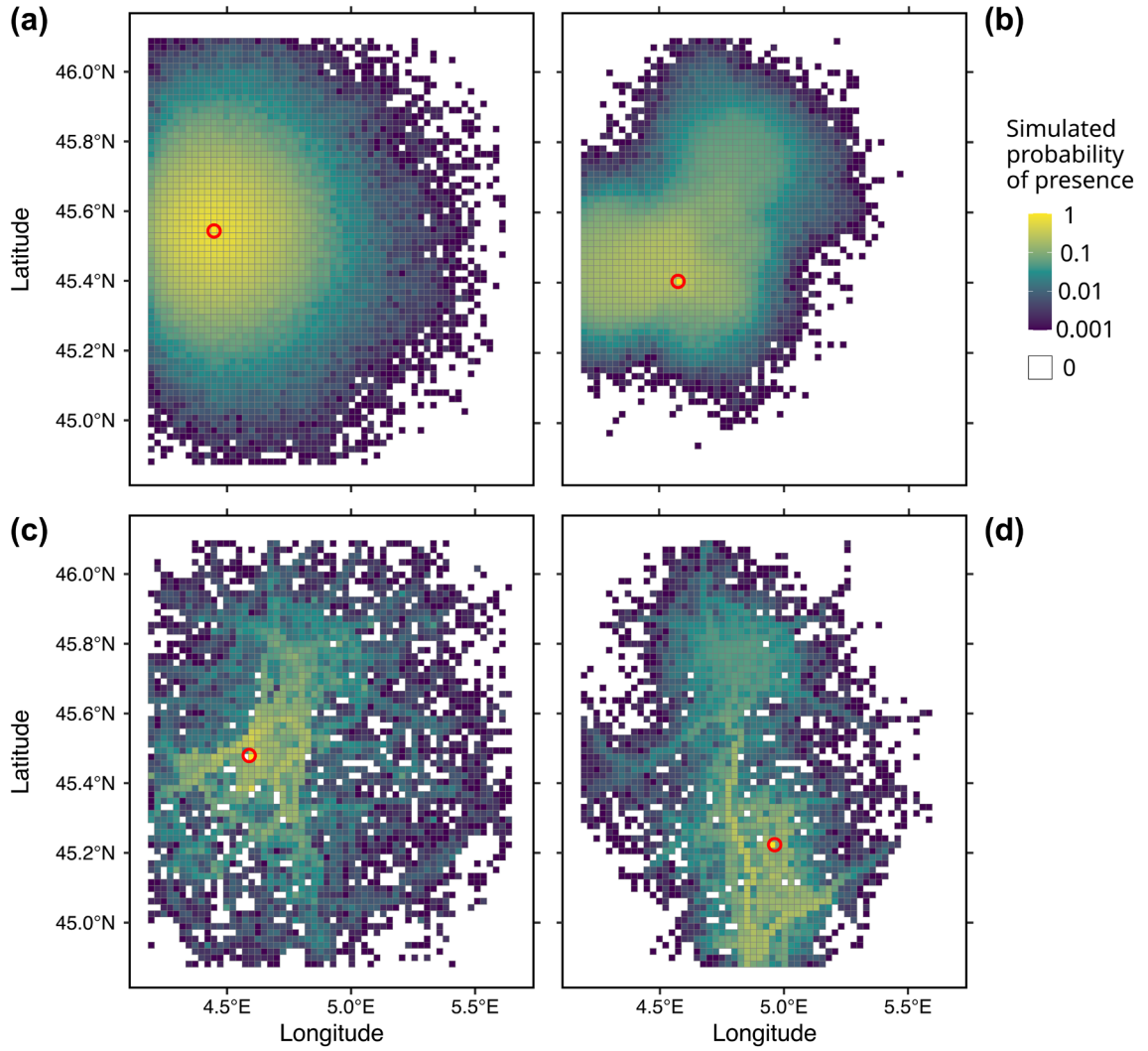

Figure 5. Simulated probabilities of presence at 25 years (based on 1000 repetitions), for each calibrated model: (a) *isotropic*, (b) *human activity*, (c) *road network* and (d) *combined*. Red circles indicate the estimated cell of introduction.

all cases. Similarly, considering only the human activity index based on population density systematically leads to poorer performances.

Moreover, our findings indicate that all roads do not participate equally to HMD as national (e.g. motorways) and regional roads were more important than smaller roads for explaining the spatial distribution of *L. neglectus* in the middle Rhône valley (Table 3, Supporting information). This result was not surprising because large roads are used by more vehicles and are therefore more likely to participate in HMD (Lemke et al. 2018). This result emphasizes the importance of anisotropy in HMD because main roads are rarer and more spatially structured in the landscape than local roads, and thus, they generate more anisotropy in HMD (Fig. 5, Supporting information for an animated version). This is in line with recent modelling studies showing that main roads participate more in the HMD of invasive animals and plants (Bagnara et al. 2022, Lee et al. 2022). However, minor roads might still play a non-negligible role by allowing isolated areas to stay connected to the main road network (i.e. large parts of the HMD trajectories occur on large roads but many HMD events start or end along smaller roads (Lee et al. 2022).

Our results also question the relevance of using human population density as a source of anisotropy in HMD models (Robinet et al. 2009, 2016, Crespo-Pérez et al. 2011). Integrating human population density in HMD models is thought to improve HMD models because human activities (that are responsible for the HMD of invasive species) are expected to be more frequent in the most populated areas (Gilbert et al. 2004). However, in our case, using human population density decreased model performance to explain *L. neglectus* invasion patterns (Fig. 3–4, Table 3, Supporting information). This result suggests that human population density is too general to properly reflect the activities involved in the HMD of the invasive ant *L. neglectus* in the study landscape, which, most likely, are local horticultural trade, landscaping and construction works (Espadaler et al. 2007, Gippet et al. 2017). If available, indices such as road traffic

density, or soil transportation activities, which are more representative of the type of human activities involved in the HMD of the studied species should be preferred in future modelling studies (Auffret et al. 2014).

Estimated parameter values also differed substantially among the four models. In this regard, the *combined* model strongly diverged from other models in its dispersal dynamics. First, the mean distance of dispersal events was twice higher than for other models ($\mu = 7.59$), and the SD of these dispersal event distances was the closest to zero ($\sigma = 0.16$), leading to long, but predictable (i.e. low variance), dispersal events. The *combined* model also strongly favored national roads while the *road network* model gave more weight to regional roads (Table 3). Moreover, while the other three models started the spread in the west area of the map (Fig. 5a–c), the *combined* model placed the introduction in the south, at ~ 15 km east from the oldest known invaded location in the study area (i.e. Saint Désirat village; Fig. 5d). The western introduction scenario is also interesting because it locates the beginning of the invasion in the middle of an historically important transportation axis (the A47 highway), connecting the two largest cities of the study area: Lyon and Saint-Etienne. Altogether, these differences show that considering the road network and the population density can strongly affect the optimal solution to explain spread patterns, and ultimately our comprehension of HMD dynamics.

One other important difference between the four models is the λ parameter value, which is the smallest for the *road network* model. This parameter controls the mean number of HMD events per year and per cell and, depending on the network connectivity, will control the intensity of the global spread. As such, the road network model simulates much less HMD events than the other models, despite having the best AIC (Supporting information). This suggests that the road network model is not only the best fitting model, but also the most parsimonious.

This study focused on how the topology of transport networks affects HMD to shape the regional spread of an invasive species. Our findings are therefore limited as we ignored other important drivers of the regional spread of invasive species: natural dispersal, biotic interactions, and abiotic conditions (Savage and Renton 2014). These factors might be particularly important for invasive species that can survive only in specific environmental conditions (Chapman et al. 2019), or with good natural dispersal abilities (e.g. the Asian hornet, *Vespa velutina*, for which HMD might be less important for post-introduction invasion success; Robinet et al. 2018). In addition, part of the population dynamics not accounted here could interact with the human-mediated dispersal process and ultimately affect spread dynamics. Among such unaccounted processes, population growth after introduction is likely important because small, incipient, populations are less likely to be dispersed by human activities than larger, older, ones. This might affect the timing of the invasion by generating a time lag between introduction and secondary human-mediated dispersal, or by inflating the importance of older populations in regional spread patterns. Future research could use our HMD model in combination to demographic sub-models (e.g. simulating population growth inside invaded cells) to address this limitations. Because our modelling framework uses parameters that are independent of the biological characteristics of the transported species (e.g. natural dispersal ability, ecological niche), it is generalizable to any species dispersed by human activities and can be coupled with species-specific models of natural dispersal and biotic or abiotic constraints (Savage and Renton 2014), allowing exploration of how HMD interacts with natural processes to shape invasion dynamics.

Conclusion

In a changing world, new roads are built at an alarming pace (Hughes 2019, Ferrante and Fearnside 2020), creating opportunities for invasive species to access pristine landscapes and facilitating their spread in urbanizing regions. Integrating road network topology in invasion models is thus crucial to understand past invasions and to prevent, future ones. Our modelling framework should stimulate ecologists and conservationists to explore the role played by road networks in driving invasive species post-introduction spread across the world's landscapes.

Acknowledgements – We wish to thank H. Berry, J. Bujan, O. Dangles, G. Fenn-Moltu, J. P. Léna, S. Ollier and T. M. Szewczyk for helpful comments on the early draft and the manuscript. We also thank N. P. Charrier for stimulating discussions and timely computer rescue.

Funding – This work was supported by the LABEX IMU (ANR-10-LABX-0088) of Univ. de Lyon, within the program 'Investissements d'Avenir' (ANR-11-IDEX-0007) operated by the French National Research Agency (ANR). It was also supported by the IXXI, Institut Rhônalpin des Systèmes Complexes. The *Lasius neglectus* sampling survey was financed by the Dépt de l'Isère and the Dépt de l'Ardèche. The IN2P3 (CNRS-USR6402) allowed us precious calculation time for testing and running our simulations. Part of the computations were performed at the Bordeaux Bioinformatics Center (CBiB).

Author contributions

Charles Rocabert: Conceptualization (equal); Formal analysis (equal); Funding acquisition (equal); Methodology (lead); Software (lead); Validation (equal); Visualization (equal); Writing – original draft (equal); Writing – review and editing (equal). **Serge Fenet**: Conceptualization (supporting); Formal analysis (supporting); Funding acquisition (equal); Methodology (equal); Resources (lead); Software (supporting); Validation (supporting); Visualization (supporting); Writing – original draft (supporting); Writing – review and editing (supporting). **Bernard Kaufmann**: Conceptualization (supporting); Data curation (lead); Formal analysis (supporting); Funding acquisition (equal); Methodology (supporting); Project administration (supporting); Supervision (supporting); Writing – original draft

(equal); Writing – review and editing (supporting). **Jerome M. W. Gippet**: Conceptualization (equal); Data curation (lead); Formal analysis (equal); Funding acquisition (lead); Methodology (equal); Project administration (lead); Software (equal); Supervision (lead); Validation (equal); Visualization (equal); Writing – original draft (equal); Writing – review and editing (equal).

Transparent peer review

The peer review history for this article is available at https://publons.com/publon/10.1111/ecog.07068.

Data availability statement

Data are available from the Dryad Digital Repository: https://doi.org/10.5061/dryad.tdz08kq5j (Rocabert et al. 2023). The simulation software developed and used for this work is freely available at https://github.com/charlesrocabert/MoRIS.

Supporting information

The Supporting information associated with this article is available with the online version.

References

Adnan, M., Gazder, U., Yasar, A., Bellemans, T. and Kureshi, I. 2021. Estimation of travel time distributions for urban roads using GPS trajectories of vehicles: a case of Athens, Greece. – Pers. Ubiquit. Comput. 25: 237–246.

Allouche, O., Tsoar, A. and Kadmon, R. 2006. Assessing the accuracy of species distribution models: prevalence, kappa and the true skill statistic (TSS). – J. Appl. Ecol. 43: 1223–1232.

Ansong, M. and Pickering, C. 2013. Are weeds hitchhiking a ride on your car? A systematic review of seed dispersal on cars. – PLoS One 8: e80275.

Ansong, M. and Pickering, C. 2014. Weed seeds on clothing : a global review. – J. Environ. Manage. 144: 203–211.

Auffret, A. G., Berg, J. and Cousins, S. A. O. 2014. The geography of human-mediated dispersal. – Divers. Distrib. 20: 1450–1456.

Bagnara, M., Nowak, L., Boehmer, H. J., Schöll, F., Schurr, F. M. and Seebens, H. 2022. Simulating the spread and establishment of alien species along aquatic and terrestrial transport networks: a multi-pathway and high-resolution approach. – J. Appl. Ecol. 59: 1769–1780.

Banks, N. C., Paini, D. R., Bayliss, K. L. and Hodda, M. 2015. The role of global trade and transport network topology in the human-mediated dispersal of alien species. – Ecol. Lett. 18: 188–199.

Bertelsmeier, C. and Courchamp, F. 2014. Future ant invasions in France. – Environ. Conserv. 41: 217–228.

Bossenbroek, J. M., Kraft, C. E. and Nekola, J. C. 2001. Prediction of long-distance dispersal using gravity models: zebra mussel invasion of inland lakes. – Ecol. Appl. 11: 1778–1788.

Bradshaw, C. J. A., Leroy, B., Bellard, C., Roiz, D., Albert, C., Fournier, A., Barbet-Massin, M., Salles, J. M., Simard, F. and Courchamp, F. 2016. Massive yet grossly underestimated global costs of invasive insects. – Nat. Commun. 7: 12986.

Bullock, J. M., Bonte, D., Pufal, G., da Silva Carvalho, C., Chapman, D. S., García, C., García, D., Matthysen, E. and Delgado, M. M. 2018. Human-mediated dispersal and the rewiring of spatial networks. – Trends Ecol. Evol. 33: 958–970.

Chapman, D., Pescott, O. L., Roy, H. E. and Tanner, R. 2019. Improving species distribution models for invasive non-native species with biologically informed pseudo-absence selection. – J. Biogeogr. 46: 1029–1040.

Crespo-Pérez, V., Rebaudo, F., Silvain, J. and Dangles, O. 2011. Modeling invasive species spread in complex landscapes: the case of potato moth in Ecuador. – Landsc. Ecol. 26: 1447–1461.

Dormann, C. F., Schymanski, S. J., Cabral, J., Chuine, I., Graham, C., Hartig, F., Kearney, M., Morin, X., Römermann, C., Schröder, B. and Singer, A. 2012. Correlation and process in species distribution models: bridging a dichotomy. – J. Biogeogr. 39: 2119–2131.

Eritja, R., Palmer, J. R. B., Roiz, D., Sanpera-Calbet, I. and Bartumeus, F. 2017. Direct evidence of adult aedes albopictus dispersal by Car. – Sci. Rep. 7: 14399.

Espadaler, X. and Bernal, V. 2020. *Lasius neglectus*, a polygynous, sometimes invasive, ant. – CREAF.

Espadaler, X., Tartally, A., Schultz, R., Seifert, B. and Nagy, C. 2007. Regional trends and preliminary results on the local expansion rate in the invasive garden ant, *Lasius neglectus* (Hymenoptera, Formicidae). – Insectes Soc. 54: 293–301.

Ferrante, L. and Fearnside, P. M. 2020. The Amazon's road to deforestation. – Science 369: 634.

Fisher, R. A. 1936. Design of experiments. – Brit. Med. J. 1: 554.

Gilbert, M., Gregoire, J.-C., Freise, J. F. and Heitland, W. 2004. Long-distance dispersal and human population density allow the prediction of invasive patterns in the horse chestnut leafminer *Cameraria ohridella*. – J. Anim. Ecol. 73: 459–468.

Gippet, J. M. W., Mondy, N., Diallo-Dudek, J., Bellec, A., Dumet, A., Mistler, L. and Kaufmann, B. 2017. I'm not like everybody else: urbanization factors shaping spatial distribution of native and invasive ants are species-specific. – Urban Ecosyst. 20: 157–169.

Gippet, J. M. W., Piola, F., Rouifed, S., Viricel, M., Puijalon, S., Douady, C. J. and Kaufmann, B. 2018. Multiple invasions in urbanized landscapes: interactions between the invasive garden ant *Lasius neglectus* and Japanese knotweeds (*Fallopia* spp.). – Arthropod Plant Interact. 12: 351–360.

Gippet, J. M. W., Liebhold, A. M., Fenn-Moltu, G. and Bertelsmeier, C. 2019. Human-mediated dispersal in insects. – Curr. Opin. Insect Sci. 35: 96–102.

Hanley, J. A. and Mcneil, B. J. 1982. The meaning and use of the area under a receiver operating characteristic (ROC) curve. – Radiology 143: 29–36.

Hansen, N., Müller, S. D. and Koumoutsakos, P. 2003. Reducing the time complexity of the derandomized evolution etrategy with covariance matrix adaptation (CMA-ES). – Evol. Comput. 11: 1–18.

Horvitz, N., Wang, R., Wan, F. and Nathan, R. 2017. Pervasive human-mediated large-scale invasion: analysis of spread patterns and their underlying mechanisms in 17 of China's worst invasive plants. – J. Ecol. 105: 85–94.

Hosmer Jr, D. W., Lemeshow, S. and Sturdivant, R. X. 2013. Applied logistic regression , Vol. 398. – JW & Sons.

Hughes, A. C. 2019. Understanding and minimizing environmental impacts of the belt and road initiative. – Conserv. Biol. 33: 883–894.

Hulme, P. E. 2009. Trade, transport and trouble: managing invasive species pathways in an era of globalization. – J. Appl. Ecol. 46: 10–18.
Hulme, P. E., Bacher, S., Kenis, M., Klotz, S., Kühn, I., Minchin, D., Nentwig, W., Olenin, S., Panov, V., Pergl, J., Pyšek, P., Roques, A., Sol, D., Solarz, W. and Vilà, M. 2008. Grasping at the routes of biological invasions: a framework for integrating pathways into policy. – J. Appl. Ecol. 45: 403–414.
Johnson, L. E., Ricciardi, A. and Carlton, J. T. 2001. Overland dispersal of aquatic invasive species: a risk assessment of transient recreational boating. – Ecol. Appl. 11: 1789–1799.
Johnson, L. E., Bossenbroek, J. M. and Kraft, C. E. 2006. Patterns and pathways in the post-establishment spread of non-indigenous aquatic species: the slowing invasion of North American inland lakes by the zebra mussel. – Biol. Invas. 8: 475–489.
Koch, F. H., Yemshanov, D., Magarey, R. D. and Smith, W. D. 2012. Dispersal of invasive forest insects via recreational firewood: A quantitative analysis. – J. Econ. Entomol. 105: 438–450.
Lee, S., Cho, H., Choi, Y., Choi, W. I., Chung, H. I., Lim, N., Nam, Y. and Jeon, S. 2022. Path-finding algorithm as a dispersal assessment method for invasive species with human-vectored long-distance dispersal event. – Divers. Distrib. 28: 1214–1226.
Lemke, A., Kowarik, I. and von der Lippe, M. 2018. How traffic facilitates population expansion of invasive species along roads: the case of common ragweed in Germany. – J. Appl. Ecol. 56: 413–422.
Lustig, A., Worner, S. P., Pitt, J. P. W., Doscher, C., Stouffer, D. B. and Senay, S. D. 2017. A modeling framework for the establishment and spread of invasive species in heterogeneous environments. – Ecol. Evol. 7: 8338–8348.
Maxwell, S. L., Fuller, R. A., Brooks, T. M. and Watson, J. E. 2016. Biodiversity: the ravages of guns, nets and bulldozers. – Nature 536: 143–145.
McNitt, J., Chungbaek, Y. Y., Mortveit, H., Marathe, M., Campos, M. R., Desneux, N., Brévault, T., Muniappan, R. and Adiga, A. 2019. Assessing the multi-pathway threat from an invasive agricultural pest: *Tuta absoluta* in Asia. – Proc. R. Soc. B. 286: 20191159.
Morel-Journel, T., Assa, C. R., Mailleret, L. and Vercken, E. 2018. Its all about connections: hubs and invasion in habitat networks. – Ecol. Lett. 22: 313–321.
Muirhead, J. R., Leung, B., van Overdijk, C., Kelly, D. W., Nandakumar, K., Marchant, K. R. and MacIsaac, H. J. 2006. Modelling local and long-distance dispersal of invasive emerald ash borer *Agrilus planipennis* (Coleoptera) in North America. – Divers. Distrib. 12: 71–79.
Perkins, T. A., Garcia, A. J., Paz-Soldán, V. A., Stoddard, S. T., Reiner, R. C., Vazquez-Prokopec, G., Bisanzio, D., Morrison, A. C., Halsey, E. S., Kochel, T. J., Smith, D. L., Kitron, U., Scott, T. W. and Tatem, A. J. 2014. Theory and data for simulating fine-scale human movement in an urban environment. – J. R. Soc. Interface 11: 20140642.
Pitt, J. P. W., Worner, S. P. and Suarez, A. V. 2009. Predicting Argentine ant spread over the heterogeneous landscape using a spatially explicit stochastic model. – Ecol. Appl. 19: 1176–1186.
Prasad, A. M., Iverson, L. R., Peters, M. P., Bossenbroek, J. M., Matthews, S. N., Davis Sydnor, T. and Schwartz, M. W. 2010. Modeling the invasive emerald ash borer risk of spread using a spatially explicit cellular model. – Landsc. Ecol. 25: 353–369.
Robinet, C., Roques, A., Pan, H., Fang, G., Ye, J., Zhang, Y. and Sun, J. 2009. Role of human-mediated dispersal in the spread of the pinewood nematode in China. – PLoS One 4: e4646.
Robinet, C., Suppo, C. and Darrouzet, E. 2016. Rapid spread of the invasive yellow-legged hornet in France: the role of human-mediated dispersal and the effects of control measures. – J. Appl. Ecol. 54: 205–215.
Robinet, C., Darrouzet, E. and Suppo, C. 2018. Spread modelling: a suitable tool to explore the role of human-mediated dispersal in the range expansion of the yellow-legged hornet in Europe. – Int. J. Pest Manage. 65: 258–267.
Rocabert, C., Fenet, S., Kaufmann, B. and Gippet, J. M. W. 2023. Data from: Accounting for the topology of road networks to better explain human-mediated dispersal in terrestrial landscapes. – Dryad Digital Repository, https://doi.org/10.5061/dryad.tdz08kq5j.
Roiz, D., Eritja, R., Escosa, R., Lucientes, J., Marquès, E., Melero-Alcíbar, R., Ruiz, S. and Molina, R. 2007. A survey of mosquitoes breeding in used tires in Spain for the detection of imported potential vector species. – J. Vector Ecol. 32: 10–15.
Rouifed, S., Piola, F. and Spiegelberger, T. 2014. Invasion by *Fallopia* spp. in a French upland region is related to anthropogenic disturbances. – Basic Appl. Ecol. 15: 435–443.
Roura-Pascual, N., Bas, J. M., Thuiller, W., Hui, C., Krug, R. M. and Brotons, L. 2009. From introduction to equilibrium: reconstructing the invasive pathways of the Argentine ant in a Mediterranean region. – Global Change Biol. 15: 2101–2115.
Savage, D. and Renton, M. 2014. Requirements, design and implementation of a general model of biological invasion. – Ecol. Modell. 272: 394–409.
Schultz, R. and Seifert, B. 2005. *Lasius neglectus* (Hymenoptera: Formicidae) – a widely distributed tramp species in Central Asia. – Myrmecol. Nachr. 7: 47–50.
Seebens, H., Schwartz, N., Schupp, P. J. and Blasius, B. 2016. Predicting the spread of marine species introduced by global shipping. – Proc. Natl Acad. Sci. USA 113: 5646–5651.
Seifert, B. 2007. Die Ameisen Mittel- und Nordeuropas. – Lutra Verlags- und Vertriebsgesellschaft, 368 pp.
Suarez, A. V., Holway, D. A. and Case, T. J. 2001. Patterns of spread in biological invasions dominated by long-distance jump dispersal: insights from Argentine ants. – Proc. Natl Acad. Sci. USA 98: 1095–1100.
Suppo, C., Robinet, C., Perdereau, E., Andrieu, D. and Bagnères, A. 2018. Potential spread of the invasive North American termite, *Reticulitermes flavipes*, and the impact of climate warming. – Biol. Invas. 20: 905–922.
Ugelvig, L. V., Drijfhout, F. P., Kronauer, D. J., Boomsma, J. J., Pedersen, J. S. and Cremer, S. 2008. The introduction history of invasive garden ants in Europe: integrating genetic, chemical and behavioural approaches. – BMC Biol. 6: 11.
Van Loon, A. J., Boomsma, J. J. and Andrasfalvy, A. 1990. A new polygynous *Lasius* species (Hymenoptera; Formicidae) from central Europe. – Insectes Soc. 37: 348–362.
Von Der Lippe, M. and Kowarik, I. 2008. Do cities export biodiversity? Traffic as dispersal vector across urban-rural gradients. – Divers. Distrib. 14: 18–25.
Zhang, L., Rohr, J., Cui, R., Xin, Y., Han, L., Yang, X., Gu, S., Du, Y., Liang, J., Wang, X., Wu, Z., Hao, Q. and Liu, X. 2022. Biological invasions facilitate zoonotic disease emergences. – Nat. Commun. 13: 1762.